Original Paper

On the interaction of glasses with high-energy radiation – Combined ESR and optical studies[1]

Marianne Nofz and Christian Reich

Bundesanstalt für Materialforschung und -prüfung, Berlin (Germany)

Reinhard Stösser and Jens Bartoll

Institut für Chemie, Humboldt-Universität, Berlin (Germany)

Eberhard Janata

Hahn-Meitner-Institut, Berlin (Germany)

This paper will discuss some aspects of the induced physical processes and chemical reactions which are observed when silicate and aluminosilicate glasses are exposed to UV radiation (248 nm; excimer laser), γ radiation (^{60}Co) and pulses of fast electrons (3.8 MeV). The stimulated emission and absorption of short-lived defects and Čerenkov radiation are detected in the optical range between 200 and 800 nm and on the microsecond time scale. Stable hole centres ($Si-O^-/h^+$, $Si-O-Al/h^+$) and electron centres (among others Zn^+, Cd^+, $(Fe^{3+})^-$) are detected by ESR spectroscopy at room temperature. They show surprising differences in regard to their thermal stability, i.e., the distribution and mean value of their trap depths. Induced absorption in the UV/VIS range exhibits broad and overlapping bands, some of which can be partially assigned to centres detected by ESR spectroscopy. Therefore, UV/VIS spectroscopy provides complementary information, an induced absorption at 300 nm for example, which has no analogy in ESR measurements.

Zur Wechselwirkung von Gläsern mit hochenergetischer Strahlung – Kombinierte ESR- und optische Untersuchungen

Am Beispiel UV- (248 nm, Excimer-Laser) und γ- (^{60}Co)bestrahlter sowie Elektronenstrahlpulsen (3.8 MeV) ausgesetzter Silicat- und Alumosilicatgläser werden einige Aspekte der induzierten physikalischen Prozesse bzw. chemischen Reaktionen diskutiert. Die Untersuchungen umfassen den optischen (200 bis 800 nm; Mikrosekunden-Bereich) Nachweis sowohl von Čerenkov-Strahlung als auch der stimulierten Emission und Absorption kurzlebiger Defekte. ESR-spektroskopisch ließen sich langlebige, d.h. bei Zimmertemperatur stabile, Loch- ($Si-O^-/h^+$, $Si-O-Al/h^+$) und Elektronenzentren (u.a. Zn^+, Cd^+, $(Fe^{3+})^-$) nachweisen. Diese zeigen überraschende Unterschiede bezüglich der thermischen Stabilität, d.h. der Mittelwerte und Verteilungen der Fallentiefen. Die UV/VIS-spektroskopische Charakterisierung der induzierten Absorption ist auf sehr breite, überlagerte Banden zurückzuführen, die teilweise ESR-spektroskopisch nachgewiesenen Defekten zuzuordnen sind. Daher liefert die UV/VIS-Spektroskopie komplementäre Aussagen, z.B. bezüglich einer Absorptionsbande bei 300 nm, die keine ESR-Entsprechung findet.

1. Introduction

The broad range of applications of glasses covers a wide variety of instances where these materials, aimed or accidentally, are exposed to different kinds of radiation. One of the largest fields is the interaction of optical materials with radiation. Thus, systematic experimental studies of irradiation-induced changes of optical properties started in the 40 s. It was the goal of the first research projects to reduce or avoid the formation of colour centres. During the next two decades numerous radiation effect studies were performed. Overviews of the results and main ideas developed up to the 80s are given in [1 and 2]. A lot of knowledge of the basic phenomena was collected including the identification of several electron and hole centres detectable by means of optical and ESR spectroscopy and its assignment to structural units of the glasses. Only a few studies were devoted to the kinetics of formation and reaction of colour and paramagnetic centres, respectively.

Nowadays, new fields of application (figure 1), especially the use of waveguides in communication systems, nuclear technology, and space research, require a knowledge in depth of relations between glass composition/local structure and parameters of radiation (e.g., energy, dose, dose rate). The resulting activities have not only to be directed to the study of the properties of

76

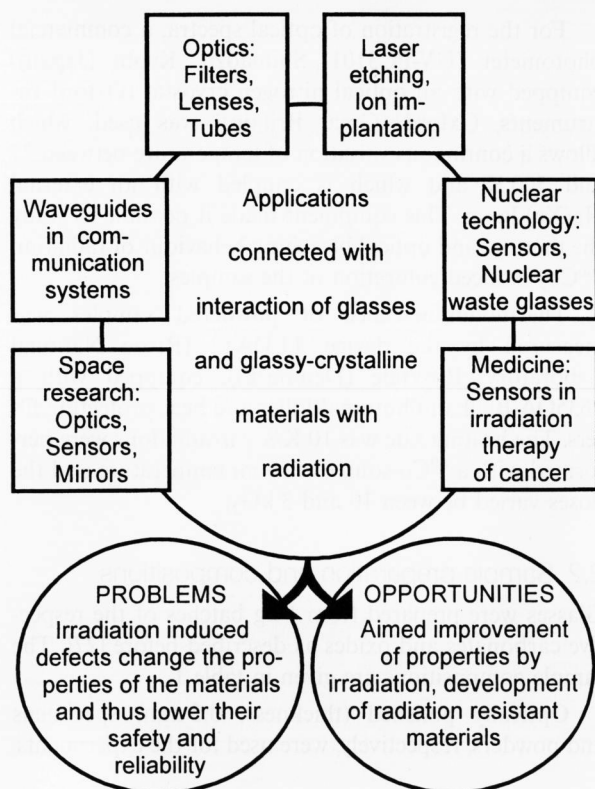Glastech. Ber. Glass Sci. Technol. 72 (1999) No. 3

Figure 1. Fields of interaction between radiation and glasses or glassy-crystalline materials and resulting problems and opportunities in materials science.

defects stable at room temperature but also to in situ investigation of the immediate processes. Thus, numerous publications appeared in the last ten years [3 to 22] which essentially dealt with

− optical fibers (e.g., SiO_2-containing different amounts of OH groups and dopants),
− SiO_2 films,
− special optical glasses used for the fabrication of lenses and filters,
− float glass,
− glass-ceramic materials with low thermal expansion (e.g. ZERODUR).

These materials interacted with γ quanta (^{60}Co, ^{137}Cs), excimer lasers (operating at 193, 248 or 308 nm), fast neutrons, electrons or protons, or ion beams.

In the present paper, selected effects of the action of UV (248 nm; excimer laser), γ irradiation (^{60}Co) and fast electrons (3.8 MeV) on silicate and aluminosilicate glasses will be discussed under physical and chemical aspects. This work includes different tasks: first, construction of suitable experimental arrangements for a sensitive and fast detection of radiation-induced changes, second, application of appropriate algorithms for utilizing the obtained data sets, and third, interpretation of the observed relations and dependencies.
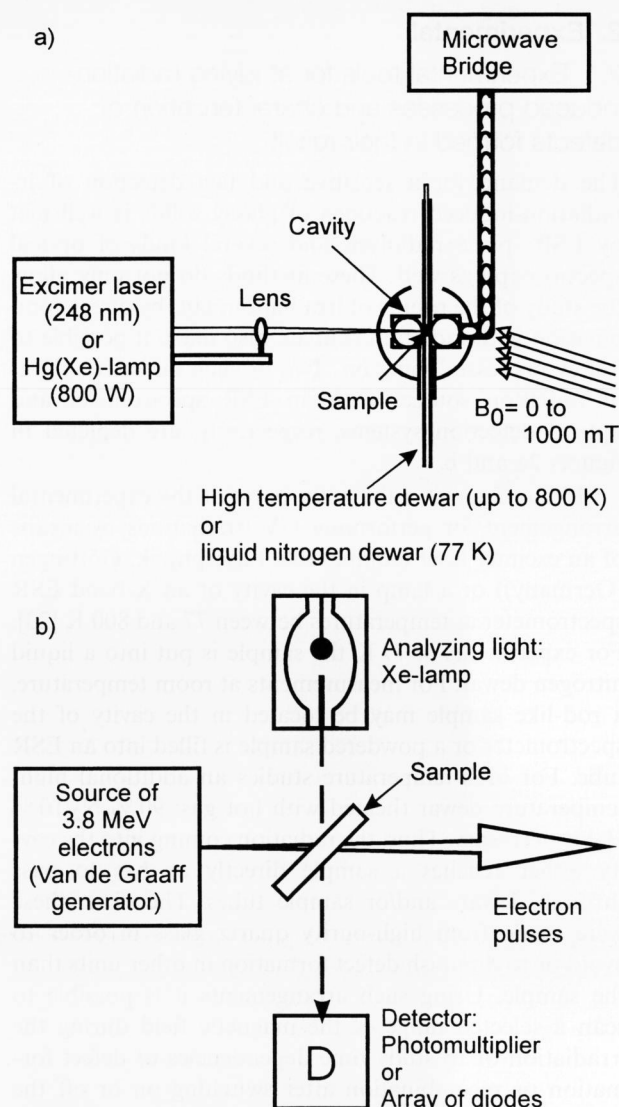
Figures 2a and b. Experimental equipment for a) in situ observation of optical and thermal bleaching behaviour in the X band ESR spectrometer, b) optical spectroscopy in the range of microseconds to milliseconds after the impact of 3.8 MeV electrons.

Table 1. Compositions of samples under consideration

sample	composition in mol %
BS	30 BaO, 70 SiO_2
CAS1	33 CaO, 5 Al_2O_3, 62 SiO_2
CAS2	30 CaO, 30 Al_2O_3, 40 SiO_2
CAS3	29 CaO, 13 Al_2O_3, 58 SiO_2
CCdAS	21 CaO, 8 CdO, 13 Al_2O_3, 58 SiO_2
CdAS	21 CdO, 21 Al_2O_3, 58 SiO_2
CZAS	21 CaO, 8 ZnO, 13 Al_2O_3, 58 SiO_2
ZAS	15 ZnO, 20 Al_2O_3, 65 SiO_2

It is the aim of this paper to show new opportunities and results as well as unresolved problems of combination of optical and ESR spectroscopy for the study of irradiation-induced changes of glasses.

2. Experimental

2.1 Experimental tools for studying radiation-induced processes and characterization of defects formed in their result

The demand for a sensitive and fast detection of irradiation-induced reactions of glassy solids is well met by ESR, pulse radiolysis and several kinds of optical spectroscopy as well. These methods do not only allow the study of the results of irradiation, but, by direct combination with radiation sources, also make it possible to follow processes going on. Two of such direct couplings of radiation sources with an ESR spectrometer and optical detection systems, respectively, are depicted in figures 2a and b.

Figure 2a shows the main parts of the experimental arrangement for performing UV irradiations by means of an excimer laser (compex100, Laserphysik, Göttingen (Germany)) or a lamp in the cavity of an X-band ESR spectrometer at temperatures between 77 and 800 K [23]. For experiments at 77 K the sample is put into a liquid nitrogen dewar. For measurements at room temperature, a rod-like sample may be located in the cavity of the spectrometer or a powdered sample is filled into an ESR tube. For high-temperature studies an additional high-temperature dewar (heated with hot gas: 90 % N_2/10 % H_2) is necessary. Thus, the radiation coming into the cavity either reaches a sample directly or has to pass through dewars and/or sample tubes. Therefore, these were made from high-purity quartz glass in order to avoid or to diminish defect formation in other units than the sample. Using such arrangements it is possible to scan a selected range of the magnetic field during the irradiation or to study time dependencies of defect formation or recombination after switching on or off the radiation sources. Additionally, it is possible to study the thermal bleaching behaviour of the defects formed under irradiation as a function of temperature and time.

Transient changes in either optical absorption or light emission, due to the impingement of pulses of high-energy electrons to the glass, are recorded at the pulse radiolysis facility ELBENA at the Hahn-Meitner-Institut, Berlin (Germany). The schematic experimental arrangement [24 to 26] is shown in figure 2b. The flat and optically polished specimens (here: $(10 \times 20 \times 0.5)$ mm^3) are mounted in such a way that the analyzing light beam samples only the irradiated portion. The high-energy electrons (3.8 MeV) are delivered by a van de Graaff electron accelerator, the pulse duration can be varied from 3 to 999 ns and the dosis from some Gy to several kGy per pulse. The changes in absorption or emission are recorded versus time at a given wavelength; a spectrum can be constructed from several kinetic curves measured at different wavelengths. For the recording from the millisecond time scale on, a diode array detector is used which allows the immediate recording of spectra (200 to 800 nm) at preset times. For the recording of the emission, the analyzing light is prohibited.

For the registration of optical spectra, a commercial photometer (UV-PC3101, Shimadzu, Kyoto (Japan)) equipped with an optical nitrogen cryostat (Oxford Instruments, Oxford (Great Britain)) was used, which allows a continuous variation of temperature between 77 and 500 K and which is coupled with an external Hg(Xe) lamp. This equipment made it possible to study the thermal and optical bleaching behaviour of radiation (^{60}Co) induced coloration of the samples.

Thermoluminescence of powdered samples was measured by the device TLDA12 (Risoe National Laboratory, Roskilde (Denmark)), equipped with a 9635QA Bialkali Photomultiplier and heat-protecting filters. The heating rate was 10 K/s. γ irradiations were performed with a ^{60}Co source at room temperature and the doses varied between 10 and 3 kGy.

2.2 Sample preparation and compositions

Glasses were prepared from 1 kg batches of the respective carbonates and oxides as described before [27]. The sample compositions are given in table 1.

Optically polished (thickness: 0.5 mm) specimens and powders, respectively, were used for the experiments.
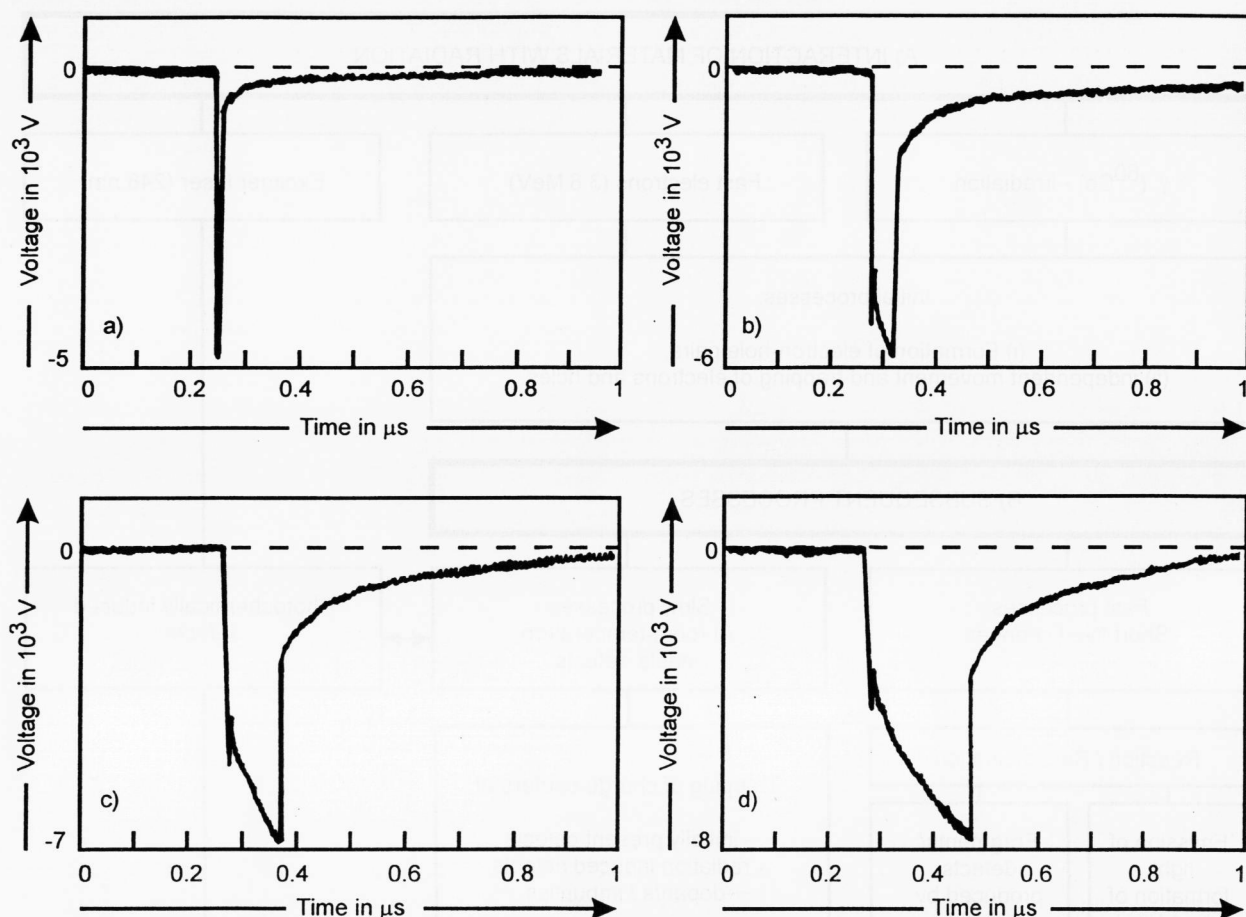
3. Physical and chemical processes induced by high-energy irradiation of solids

The scope of the experimental work to be presented here is outlined in figure 3. As shown in part A) the interactions of glassy materials with γ radiation, fast electrons and UV rays supplied by an excimer laser were studied.

The γ quanta provided by a ^{60}Co source possess an energy of 1.17 and 1.33 MeV [28]. Most of them pass through a solid material, i.e., the probability of interaction is low [2]. If interactions appear, i.e., γ quanta are absorbed, then three processes, depending on the energy of the γ quanta and on the atomic number of the absorbing atom, may appear: first, Compton recoil, second, photoelectric effect, and third, electron-positron pair formation. All these processes lead to the formation of recoil electrons (and positrons) which interact with the glass in the same way as any other energetic electron [2]. Thus, for an understanding of mechanisms of interaction of electrons with solids it is necessary to explain the results of radiation damage by γ rays and fast electrons as well.

Interaction of high-energy electrons (e.g., supplied by an accelerator or formed after interaction of a solid with γ radiation) with electrons of the lattice leads to formation of electron-hole ionization pairs. Sufficiently energetic electrons also can displace atoms. But, for MeV electrons the displacement process appears to be relatively inefficient. Thus, the main effects to be discussed in this work are the formation of electron-hole pairs, and the independent movement and trapping of electrons and holes leading to more or less stable colour centres and paramagnetic defects, respectively. The re-

A) INTERACTION OF MATERIALS WITH RADIATION

| γ (^{60}Co) - irradiation | Fast electrons (3.8 MeV) | Excimer laser (248 nm) |

Initial processes:

(i) Formation of electron-hole pairs,
(ii) independent movement and trapping of electrons and holes.

B) SUBSEQUENT PROCESSES

Fast processes:
Short-lived changes

Slow processes:
At room-temperature
stable defects

**Photochemically induced
defects**

Reaction / Recombination

Emission of light, formation of short-lived defects

Fragments/ defects produced by radiation chemistry

Trapping of charge-carriers at

- initially present defects
- radiation induced defects
- dopants / impurities

Optical spectroscopy in the range of μs
(figs. 4, 5)

UV/VIS-NIR spectroscopy
(fig. 6)

cw - X-band - ESR spectroscopy
(fig. 7)

C) POST-IRRADIATION TREATMENTS

Optical bleaching
(fig. 8)

Thermal bleaching
(fig. 9)

Thermoluminescence
(fig. 10)

Figure 3. Schematic representation of radiation-induced processes and reactions as well as post-irradiation treatments of the glasses under consideration and indication of the suitable experimental tools.

lated reactions leading to trapping, detrapping, reaction or recombination of holes and electrons (see part B) of figure 3) can be classified by the time scale of their detection at room temperature. A process shall here be called "fast" if the irradiation-induced emission or change of absorption is detectable in the time range of microseconds only. Examples of detecting such short-lived defects will be given in figures 4a to d and figure 5.

Alternatively, and as often discussed changes in the literature, the formation of colour centres and paramagnetic defects stable at room temperature was studied. These investigations include the assignment of the observed species to charge carriers trapped at initially present defects in the glass network, b) radiation-induced defects, and c) easily reducible or oxidizable dopants or impurities. An example for the discussion will

Glastech. Ber. Glass Sci. Technol. 72 (1999) No. 3

79

Marianne Nofz; Christian Reich; Reinhard Stösser; Jens Bartoll; Eberhard Janata:

Figures 4a to d. Time-resolved optical emission of sample BS for different pulse lengths, a) 10 ns, b) 50 ns, c) 100 ns, d) 200 ns.
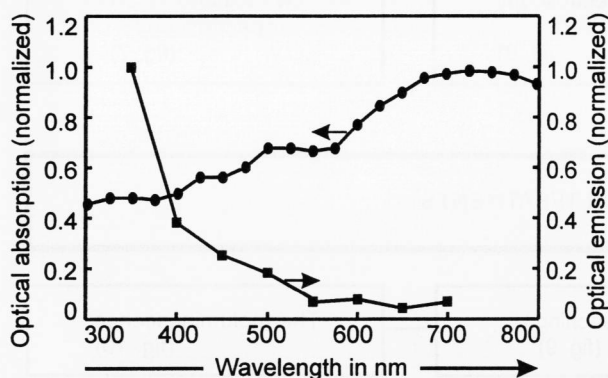

Figure 5. Irradiation-(3.8 MeV electrons) induced optical absorption and emission of sample BS taken $5.5 \cdot 10^{-7}$ and $4 \cdot 10^{-7}$ s, respectively, after 200 ns pulses.

be given with the spectra depicted in figures 6a and b, 7a and b.

Excimer laser excitation of glasses may cause photochemical reactions which can finally result in the formation of the same types of stabilized colour centres and paramagnetic defects as observed after γ or electron irradiations (figures 7a and b).

To characterize different radiation-induced defects not only their spectroscopic properties have to be studied. Their optical (figures 8a and b) and thermal (figures 9a to c and 10) bleaching behaviour can also yield valuable information to support assignments given, or to evaluate the possibility of application of materials for special purposes (e.g., applications in the fields of high-energy radiation sources).
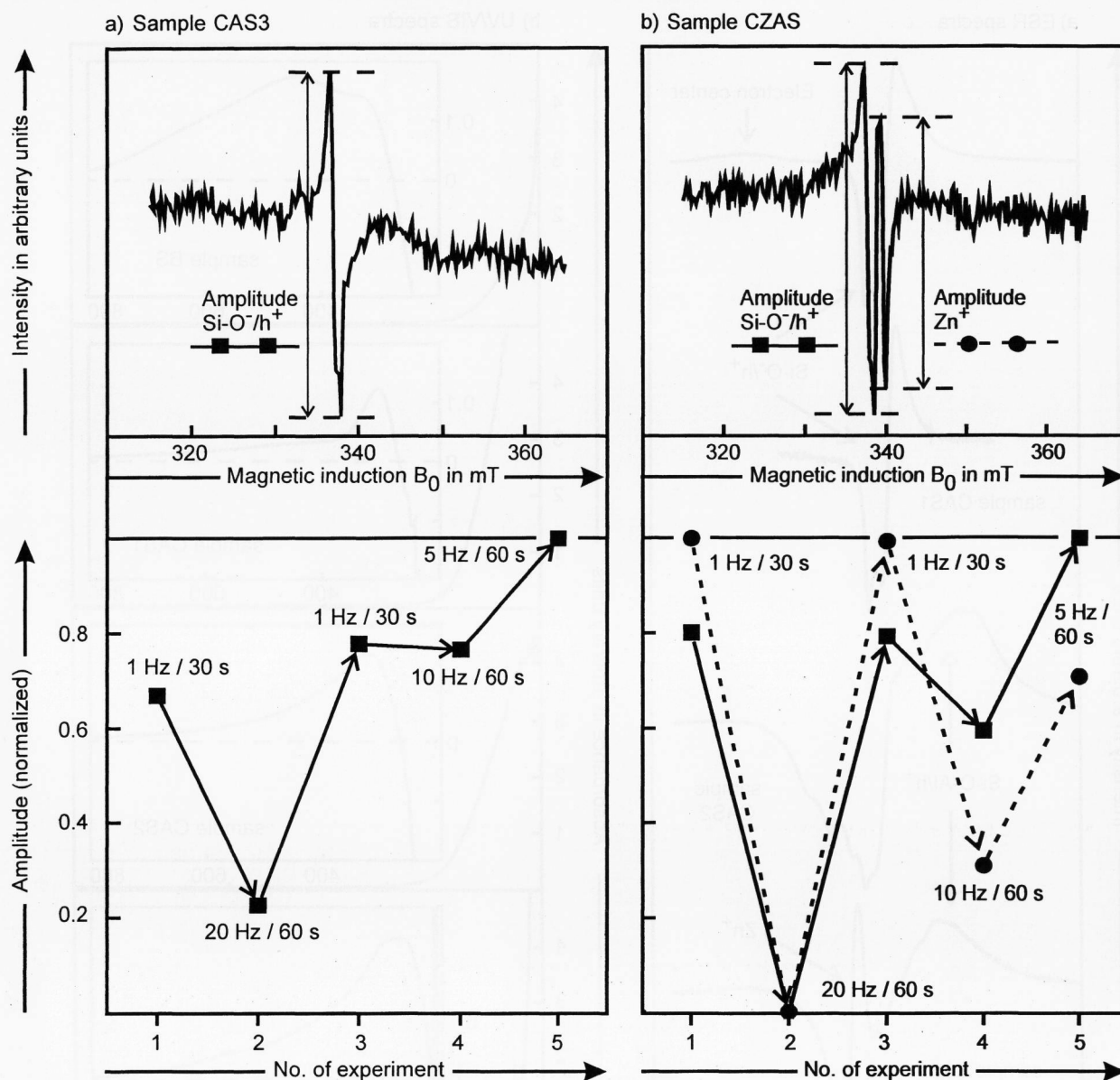
4. Results

4.1 Indication of recombination processes and detection of short-lived defects by optical spectroscopy in the range of microseconds

Figures 4a to d show the dependence of emission at 340 nm of sample BS on the pulse length. At the time scale as used the interaction of the sample with the pulses starts at 2.2 µs. At this time immediately Čerenkov radiation [29] can be detected. The intensity of this emission is approximately equal to 4.5 mV independent of the pulse length. This type of emission is always observable if electrons move through a substance with a velocity greater than that of light in the same one. Čerenkov radiation shows characteristic peculiarities which differ

80

Glastech. Ber. Glass Sci. Technol. 72 (1999) No. 3
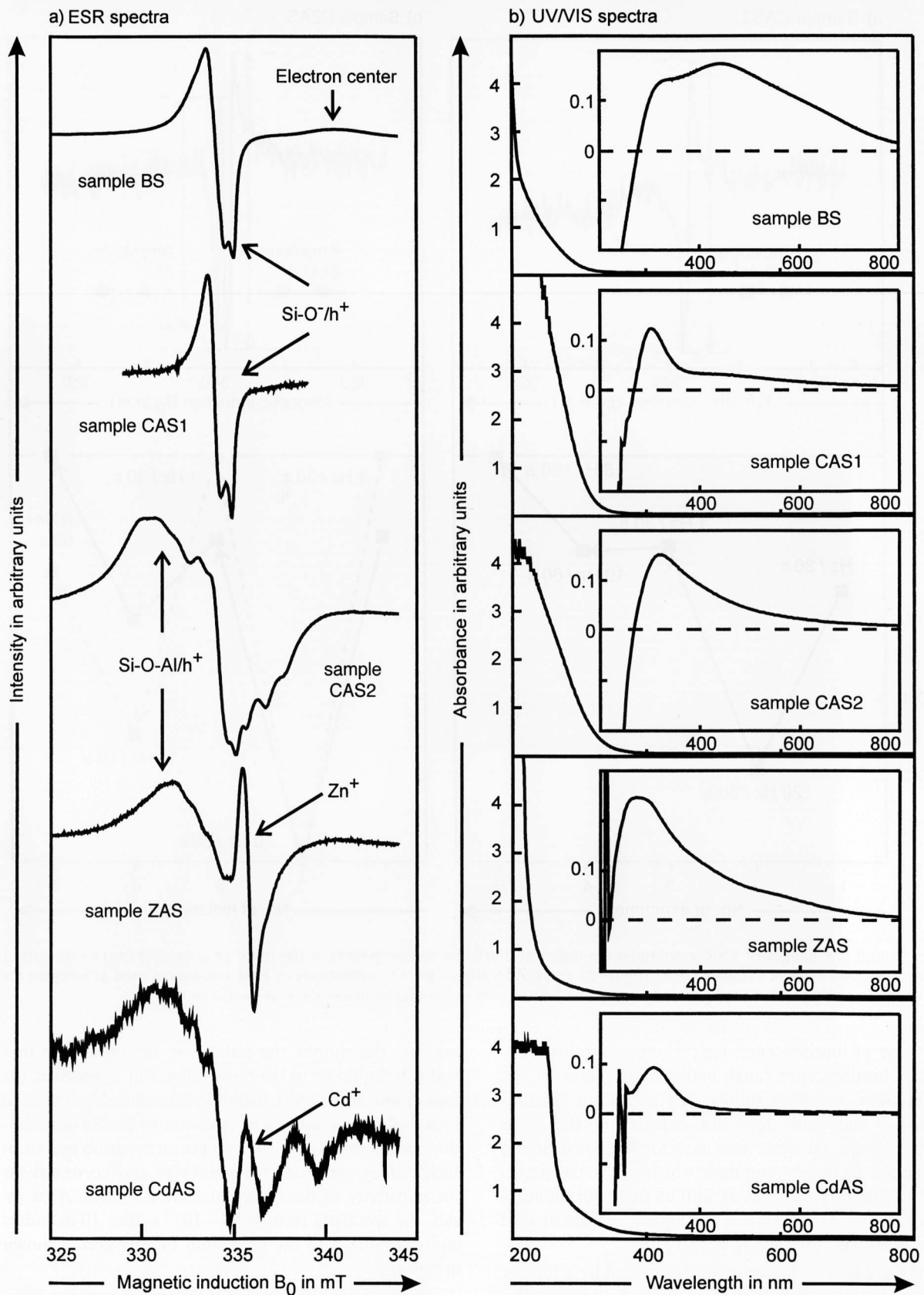
Figures 6a and b. Dependence of ESR and optical absorption of long-lived defects on the chemical composition (BS, CAS1, CAS2, ZAS, CdAS). The ESR spectra (figure a) were taken at room temperature at 20 mW microwave power. UV/VIS spectra (figure b) show the absorbance of the samples referenced to air; the inserts depict the radiation-induced absorption, i.e., the spectra of the irradiated samples were taken using the unirradiated ones as references.

Glastech. Ber. Glass Sci. Technol. 72 (1999) No. 3

81

Marianne Nofz; Christian Reich; Reinhard Stösser; Jens Bartoll; Eberhard Janata:

Figures 7a and b. Changes of ESR amplitudes (recorded at 2 mW microwave power) in the result of laser (248 nm) treatments at different repetition rates of samples CAS3 (figure a) and CZAS (figure b). The amplitudes of ESR resonances used as measure for the effect of laser irradiation are indicated above. The lines drawn in the graphs below serve as guides to the eye.

from those of luminescence, e.g., whereas the time constants of luminescence range between 10^{-7} and 10^{-8} s, the Čerenkov radiation follows the excitation "instantaneously" and thus does not depend on the pulse length. This special effect was used for the construction of so-called Čerenkov counters which allow the detection of single fast particles as well as the determination of their energy. These devices use liquids, acrylic or lead silicate glasses as interacting media [30].

The Čerenkov radiation is superimposed by a further emission. Its intensity depends on the pulse length. The decay of this emission can be described by second-order kinetics and yields first half-life times which depend on the pulse length as summarized in table 2. This dependence is an artefact caused by the concurrent decay and initiation of emission processes during the pul-

ses, i.e., the shorter the pulses are the closer the first half-life should be to the right value. But in practice, the lower limit of the pulse length is determined by the need to stimulate a minimum of emission to enable quantitative measurements. In order to get an emission spectrum such curves were detected pointwise and corrected for the sensitivity of the optical detection system. As a result, the spectrum recorded $4 \cdot 10^{-7}$ s after 10 ns pulses and normalized to the maximum of emission is shown in figure 5.

Figure 5 also depicts a normalized absorption spectrum of a sample of the same composition also detected in the time range of microseconds ($5.5 \cdot 10^{-7}$ s). Three features have to be mentioned: first, the spectra are composed of very broad and superimposed absorption bands, second, the maximum absorption appears at

a) ESR spectroscopy

b) UV/VIS spectroscopy
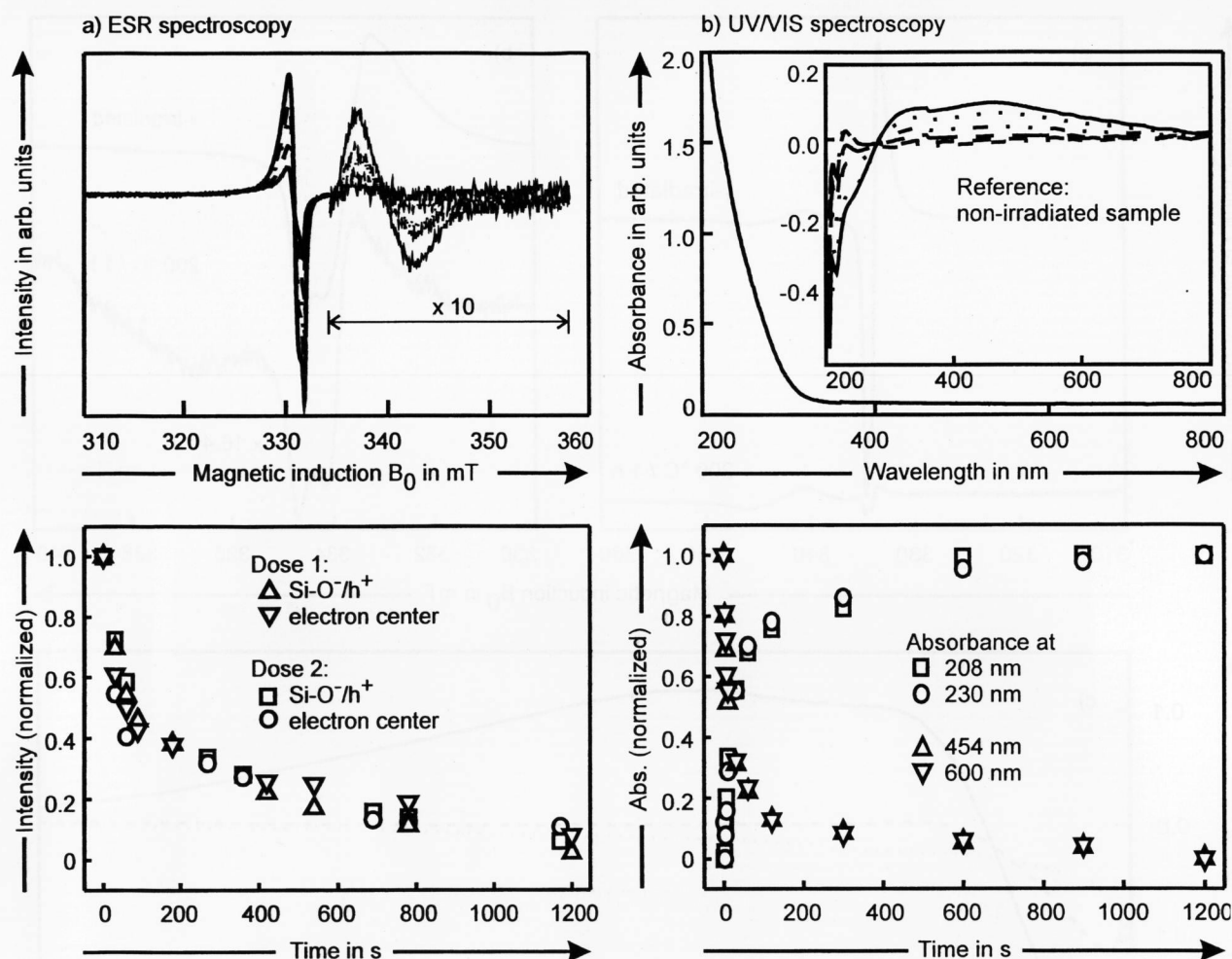
Figures 8a and b. ESR (figure a) and UV/VIS (figure b) spectroscopic study of optical bleaching with the light of a Hg(Xe)lamp (800 W) at 77 K of γ-irradiated (300 K, dose 1: 2.5 kGy, dose 2: 5.8 kGy) sample BS. Selected ESR and UV/VIS spectra were depicted above to give an impression of observable changes. (Please note that the amplitudes of the ESR signals belonging to electron centres were scaled by factor 10). The time dependencies , i.e., the plot of normalized amplitudes of ESR resonances and optical absorption at selected wavelengths versus duration of bleaching, obtained for the whole series of experiments are plotted in the bottom part of the figure. In figure b) the absorption of the non-irradiated sample (reference: air) is also shown. Full line: γ-irradiated samples, dashed lines: γ-irradiated and subsequently bleached samples.

wavelengths greater than 600 nm, and third, in contrast, the maximum of emission was detected at short wavelengths ($\leq$300 nm) and for $\lambda \geq$ 550 nm no emission could be detected. The absorption at 450 nm versus time curve (not shown here) follows a second-order law; the first half-life is in the order of 1 to 2 · 10^{-6} s. But it has to be taken into consideration here that spontaneous recombination processes and optically stimulated ones (by the analyzing light) occur simultaneously.

This section was devoted to one binary silicate glass in order to explain main features of the detection of fast processes. Some further examples, which concern the influence of glass composition are discussed in [31 and 32].

4.2. UV/VIS-NIR and ESR spectroscopic characterization of long-lived defects

Figure 6a shows ESR and optical spectra of various glass samples obtained a long time (several days) after

γ irradiation performed at room temperature. The ESR spectra allow an assignment of the signals to distinct hole and electron traps being part of the glassy networks. If considerable amounts of nonbridging oxygens are present then they usually act as effective hole traps. This is also observed for samples BS and CAS1 (table 1) here. The ESR spectra yield characteristic patterns in the $g' \approx 2$ region. As shown in [33 and 34], they result from at least two superimposed signals. Griscom [35], in addition, also discusses the presence of E′ centres. The incorporation of a certain amount of Al_2O_3 into a silicate glass system leads to formation on Si−O−Al bridges which also, competing with the nonbridging oxygens [36], can serve as hole traps. Their identification is possible if the ^{27}Al hyperfine structure can be resolved [27 and 36]. In the glasses discussed up to here it could be shown [37 and 38] that Fe^{3+} ions serve as electron traps. Otherwise, if Cd^{2+} or Zn^{2+} ions are constituents of the glasses under consideration these ions may also yield
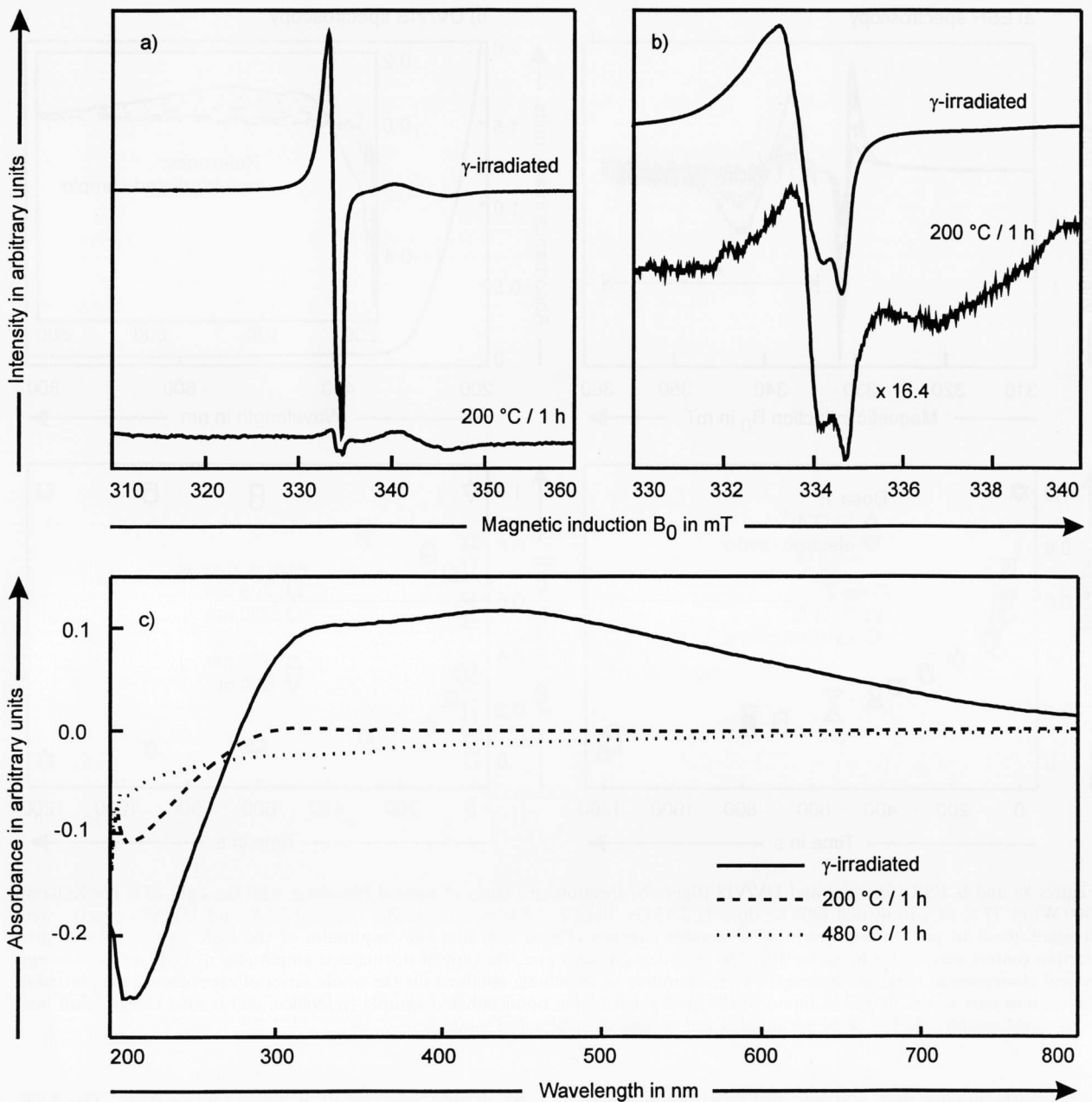
Figures 9a to c. Thermal bleaching (at 200 °C for 1 h after a period of 2 h for rising the temperature from 25 to 200 °C) of hole and electron centres indicated by ESR (figures a and b: microwave power applied = 20 mW) and corresponding optical difference spectra (figure c) of sample BS. All spectra, i.e., ESR and optical ones, were recorded at room temperature using the same specimen.

electron traps and the resulting centres often were denoted as Cd^+ and Zn^+ [1 and 31]. But, as argued in [39] the latter one could also be an oxygen vacancy. In the case of sample BS a further type of paramagnetic electron centre appears, which will be described below in more detail.

Figure 6b contains UV/VIS spectra of nonirradiated samples and, as inserts, the change of optical absorption induced by γ irradiation. The position and shape of the UV edge is different for all samples here. It depends on the total amount of iron in the sample, on the redox states and on the type of cation present, but these relations shall not be studied here. To understand the

experiments under discussion here, it is only necessary to know that the UV edge is due to $Fe^{3+}-O$ charge transfer bands. After γ irradiation the absorption in the region of the UV edge decreases for samples BS, CAS1 and CAS2, thus indicating the radiation induced reduction of a part of Fe^{3+} ions. In contrast, for the zinc- and cadmium-containing glasses such a decrease is not clearly detectable. These observations correspond with earlier ESR results [37], where similar behaviour was detected for the Fe^{3+} resonance at $g' \approx 4.3$.

The shape of the induced absorption in the visible is determined by broad and superimposed bands, which only allow to mention two distinct maxima at 300 and
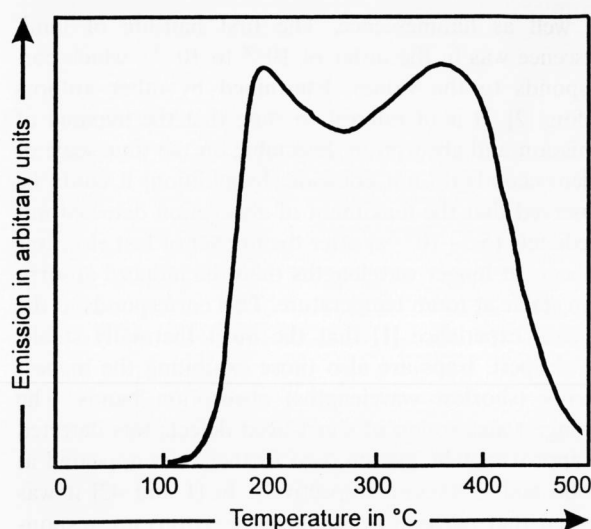
84

Glastech. Ber. Glass Sci. Technol. 72 (1999) No. 3

Figure 10. Thermoluminescence curve of γ-irradiated (2.5 kGy; 300 K) BS powder. The heating rate was 10 K s^{-1}.

Table 2. First half-life times of emission at 340 nm obtained after four different experiments at sample BS

pulse length in ns	first half-life times in s
10	$3.5 \cdot 10^{-8}$
50	$6.7 \cdot 10^{-8}$
100	$1.2 \cdot 10^{-7}$
200	$2.5 \cdot 10^{-7}$

500 nm, respectively. Their ratios change in dependence on the composition. But it has to be stressed that from this study of dependence on composition no assignment of the optical absorption maxima to the ESR resonances described before is possible.

ESR spectra of selected samples which were exposed to excimer laser radiation (248 nm) at 300 K are mirrored in figures 7a and b. The top parts show spectra obtained after 30 s of irradiation with a repetition rate of 1 Hz and indicated measures used for the quantification of induced changes of signal amplitudes. The experiments were performed in the following manner: At first spectra of the non-irradiated samples were recorded to be sure that there was no signal detectable in this region before interaction with laser radiation. Then five different irradiations were performed (bottom parts in figures 7a and b); i.e., the laser was operated (I) at 1 Hz for 30 s, (II) at 20 Hz for 60 s, (III) again at 1 Hz for 30 s, (IV) at 10 Hz for 60 s, and (V) at 5 Hz for 60 s. After each train of laser pulses ESR spectra were taken. As can be seen from this figure, after the first train of pulses a certain amount of paramagnetic centres was formed and stabilized in both samples. But after additional irradiation for 60 s at 20 Hz the signals vanished partly for sample CAS3 and completely for sample CZAS. Repeated treatment at 1 Hz for 30 s again caused formation of defects which were partly removed in

sample CZAS and did practically not change for sample CAS3 after treatment at 10 Hz. After additional irradiations at 5 Hz the concentrations of the paramagnetic centres detected in both samples before increased. It has to be stressed that for sample CZAS the ratio of the Si$-$O$^-$/h$^+$ to Zn$^+$ centres is a function of the repetition rate of the laser.

4.3 Optical and thermal bleaching behaviour of γ-irradiated samples

Figures 8a and b show results of optical bleaching experiments performed on γ-irradiated samples having the composition BS. The ESR spectrum obtained after γ irradiation shows the Si$-$O$^-$/h$^+$ resonance(s) and a broad and asymmetric signal of an electron centre. The registration of the first spectrum in each bleaching series was started together with the exposition of the sample to the light of an Hg(Xe) lamp (800 W) and the whole series of spectra was recorded continuously to ensure an unchanged position of the sample in the cavity of the ESR spectrometer. The sample was kept at 77 K for the whole time. In the result of optical excitation the amplitudes of both signals became smaller and after 30 min they were beyond detection. Following the decay of both signals for two samples irradiated with different doses the time dependencies shown below the spectra were obtained. These "intensities" were calculated from the signal amplitudes which were normalized in the way that they were equal to 1 for the first spectrum and 0 after the resonances vanished in the course of experiments. It can be seen here that no distinct dose dependence is detectable. But, looking at the ESR spectra obtained during the first 40 s it becomes obvious that the electron centres decay faster under the influence of the light of the Hg(Xe) lamp than the hole centres.

In figure 8b results of UV/VIS spectroscopic study concerning optical bleaching of sample BS are visualized. Since in the sample iron impurities are present absorption before γ irradiation is characterized by an UV edge caused by superimposed bands of Fe^{2+}$-$O (210 nm, extinction coefficient $\varepsilon \approx 3000$) and Fe^{3+}$-$O (230 nm, $\varepsilon \approx 7000$) charge transfer transitions [40 and 41]. The spectra of the sample which was irradiated and subsequently bleached at 77 K were referred to a non-irradiated sample kept at room temperature[2]. After γ irradiation (full line) the absorbance below 280 nm decreases, but increases above this wavelength. The decrease in the UV range can be explained by irradiation-induced reduction of Fe^{3+} ions which was also proven by ESR spectroscopy yielding a decrease of the amplitude of the Fe^{3+} resonance at $g' = 4.3$ as already mentioned. The induced absorption above 280 nm is due to the formation of colour centres which are characterized

---

[2] Since the additional light from the Hg(Xe) lamp would disturb the spectra registration, the sample was exposed to it for certain periods and after each one a spectrum was recorded on shielding the photometers sample compartment from the light outside.

Marianne Nofz; Christian Reich; Reinhard Stösser; Jens Bartoll; Eberhard Janata:

by very broad and superimposed bands. Thus, only a maximum at 450 and a shoulder at 300 nm could be discovered. The time dependence of the bleaching is illustrated for selected wavelengths.

Figures 9a to c show results which were obtained after thermal bleaching experiments at samples of composition BS. It has especially to be stressed here that the ESR and UV/VIS spectra were recorded at identical samples. To do so a special ESR cavity was used which allowed to place in flat samples with an area of $(10 \times 20) \, mm^2$. At first spectra of the γ-irradiated sample were recorded and then thermal treatments of the irradiated sample were performed at 200 and 480 °C, respectively, in an external furnace. Spectra were recorded after each thermal treatment again. As could be shown by ESR spectroscopy (figure 9a) an unexpected response to the temperature-time regime applied was observed which was different for electron and hole centres. The latter experience a large loss of intensity. It was also observed that the shape of the $Si-O^-/h^+$ resonance did not change significantly as a result of temperature treatment (figure 9b). After thermal bleaching at 480 °C the ESR resonances were not detectable any longer. This agrees with the findings of optical spectroscopy. Three characteristics of optical spectra can be elucidated from figure 9c: first, the absorption below 280 nm increases again after thermal treatment, i.e., reoxidation of Fe^{2+} ions (here $(Fe^{3+})^-$ ions formed in the irradiation process are meant) appears, thus supplying electrons which can be (re)trapped or react with holes; second, the absorption at 300 nm is more thermally stable than that at longer wavelengths, and third, the absorption in the visible range of the spectrum is nearly bleached out at 200 °C.

As a further proof of defects differing with respect to thermal stability, thermoluminescence, i.e., detection of thermally stimulated emission in the visible as a function of temperature, was used. Figure 10 shows the corresponding curve for sample BS. Indeed, it is characterized by two (well) separated maxima appearing at 190 and 360 °C and pointing to the presence of irradiation-induced centres of different thermal stabilities as expected from the experiments described before.

5. Discussion

5.1 Detection of fast processes and short-lived defects

The processes to be considered in this section are connected with trapping and reaction, respectively, of holes and electrons. According to [2] holes are usually trapped more quickly than electrons. Electrons can not only be trapped but also react with trapped holes and vice versa. Such recombination processes can be accompanied by emission of light or radiation. The sample of composition BS which served as example for the detection of fast processes and description of the experimentally accessible phenomena here, emitted Čerenkov radiation

as well as luminescence. The first half-life of luminescence was in the order of 10^{-8} to 10^{-7} s which corresponds to the values determined by other authors before [2]. It is of interest to state that the maxima of emission and absorption detectable on the time scale of microseconds do not coincide. In addition, it could be observed that the maximum of absorption detected immediately ($5.5 \cdot 10^{-7}$ s) after the impact of fast electrons appears at longer wavelengths than the induced absorption stable at room temperature. This corresponds to the general experience [1] that the most thermally stable, i.e. deepest, traps are also those exhibiting the highest energy (shortest wavelengths) absorption bands. The strongest absorption of short-lived defects was detected at approximately 700 nm, two further ones appeared at ≈ 500 and ≈ 300 nm, respectively. In [1 and 42] it was argued that released or stabilized electrons are responsible for absorption bands in the wavelength region 500 to 700 nm. Such an assignment is also possible for the sample BS. Bearing in mind the principle of maintaining electrical neutrality of the sample, the decay of absorption ascribed to reaction of released electrons should be accompanied by a decrease of absorption caused by trapped holes. Their absorption bands should also appear in the visible as additional superimposed bands.

From the practical point of view, i.e., evaluation of radiation hardness [10], special attention should be paid to the fact that absorption bands of short- and long-lived defects do not only differ regarding intensity but also with respect to the position of the bands.

5.2 Nature and properties of long-lived defects

Before starting a discussion directed to assignment of both, induced ESR resonances as well as optical absorption bands, it seems to be useful to describe potential types of electron and hole traps in glasses. According to their chemical nature they can be divided into two groups:

a) Traps formed by constituents of an only slightly perturbed glassy network. With respect to the samples under consideration here, such traps are

− nonbridging oxygens $Si-O^-$,
− bridging oxygens $Si-O-Si$ or $Si-O-Al$: according to ESR findings [43] and also based on consideration of charge distribution [44] only the latter act as effective hole traps competing with nonbridging oxygens,
− ions like Cd^{2+} or Zn^{2+} which are main components of the glasses and are reducible to form Cd^+ or Zn^+ and thus appear as electron traps,
− traces of Fe^{3+} and Fe^{2+} ions being part of the raw materials used for glass production and able to trap electrons and holes, respectively.

b) Traps due to point defects of a real glass network which might be formed during production of glassy materials or via atomic displacements caused by interaction of samples with highly-energetic radiation. They can be analogies to those occurring in crystals, e.g., oxy-

Table 3. Assignments of optical bands to radiation-induced defect centres given in the literature

wavelength	peculiarities	reference
electron centres		
235 to 305 nm	electrons in deeper traps	[1]
230 nm	trapped electrons; more intense in samples prepared under reducing conditions	[48]
310 nm	trapped electrons; consists of three bands, positions vary with the alkali ion present	[48]
335 nm	trapped electrons	[49]
387 nm	trapped electrons; detectable if γ dose exceeds 100 kGy	[49]
600 to 700 nm	shallow electron traps	[1]
UV, some intensity tailing into visible range of the spectrum	Zn^+, Cd^+	[1]
hole centres		
302 nm	hole centres in alkali silicate glasses	[49]
460 and 630 nm	$Si-O^-/h^+$; band position and intensity vary with alkali ion present	[1 and 48]
460 nm	aluminium—oxygen hole centre in quartz	[48]
517 nm	hole centres in alkali silicate glasses	[49]
550 nm	aluminium—oxygen hole centre in glasses	[1]
620 nm	hole centres; band position and intensity vary with alkali ion present; consists of many superimposed components	[1]
620 nm	aluminium—oxygen hole centre in quartz	[48]
670 nm	aluminium—oxygen hole centre in SiO_2 glass	[50]

gen vacancies or "interstitial" ions. As examples, defects of the type Si—Si and Si—O—O—Si providing precursors for paramagnetic E' centres or peroxy radicals in SiO_2 glasses [45] shall be mentioned here.

The close relation between chemical composition and ESR spectroscopically detectable radiation-induced defects often observed [27 and 43] for silicate and aluminosilicate glasses favours, in the work presented here, the consideration of traps belonging to group a).

Studies of the influence of composition on radiation-induced formation of paramagnetic centres and changes of optical absorption characteristics as well as results of different post-irradiation treatments, i.e., thermal and optical bleaching procedures, yielded a lot of alone standing facts. It shall be examined now to what extent they correspond to each other and to the results obtained by other authors. As mentioned above when describing the ESR spectra depicted in figures 6a and b the following types of paramagnetic centres were detected here: a) holes trapped either at non-bridging oxygens ($Si-O^-/h^+$) or at Si—O—Al bridges ($Si-O-Al/h^+$), b) electrons trapped by Zn^{2+}, Cd^{2+} being constituents of the glasses, c) electrons trapped by Fe^{3+} ions, d) trapped electrons causing an asymetrically-shaped resonance at $g' \approx 1.955$ in sample BS; similar ones were also observed in γ-irradiated strontium silicate and calcium aluminosilicate glasses [46 and 47]. Proposals for assignments of optical bands to hole and electron centres collected in table 3 were given by [1, 38 and 48 to 50].

The optical difference spectra shown in figures 6a and b are characterized by a decrease of absorption below 280 nm which indicates reduction of Fe^{3+} by trapping of electrons also detectable by ESR spectroscopy

[46]. The induced absorption, though comprising the range between 280 and 800 nm, does not show more than two separated maxima. These appear near 300 and 500 nm, respectively. The absorption band at ≈ 300 nm was also detectable for further γ-irradiated aluminosilicate glasses and vanishes at thermal treatments performed at temperatures above 150 to 550 °C (depending on glass composition [46 and 51]). It should be caused by electrons in comparatively deep traps as observed for sodium disilicate glasses before [1]. Comparison of ESR spectra of similar samples did not yield a corresponding resonance.

The irradiation-induced absorption at longer wavelengths and the decrease of absorption below 280 nm are thermally stable only below 200 °C and should be caused by further types of electron centres and by hole centres as well. $Si-O-Al/h^+$ centres were detected by ESR for samples CAS2, ZAS and CdAS. But a corresponding characteristic absorption which should not appear in the UV/VIS spectra of nonirradiated samples BS and CAS1 could not be determined here. Additionally, optical and thermal bleaching experiments did not allow one to distinguish between different types of hole centres. In [52] it had been described for CAS glasses that the thermal bleachings of $Si-O^-/h^+$ and $Si-O-Al/h^+$ observed by ESR are close together if both types of trapped holes are likewise present. This led to the conclusion that holes could undergo coupled detrapping and trapping reactions at thermal treatments performed in the range of 200 °C. Remembering the above-mentioned (section 5.1) relation between trap depth and position of absorption bands and observing very broad and superimposed ones here, it has to be assumed that for the samples under consideration the differences of trap depths are very

Glastech. Ber. Glass Sci. Technol. 72 (1999) No. 3

87

Marianne Nofz; Christian Reich; Reinhard Stösser; Jens Bartoll; Eberhard Janata:

small. But thermoluminescence made it possible to discover two well-separated maxima at 200 and 360 °C figure 10). The experiments described in figures 9a to c allow one to draw the conclusion that detrapping of holes and electrons absorbing in the visible occurs at 200 °C. Electrons in deep traps causing a resonance at $g' = 1.955$ in the ESR spectra and further ones absorbing at 300 nm should be the ones with the higher thermal stability.

Special attention has to be paid to the UV/VIS spectra obtained for γ-irradiated samples ZAS and CdAS. They do not show a decrease of absorption below 280 nm as observed for the other three samples. This difference can rest on the following peculiarities: first, formation of Cd^+ and Zn^+ causes generation of absorption bands in the UV region [1], thus, compensating the decrease of absorption caused by reduction of Fe^{3+} ions, and second, Fe^{3+} and Zn^{2+}/Cd^{2+} compete for electron trapping, thus, only a comparably small percentage of Fe^{3+} ions will be reduced. The last idea is supported by ESR study of radiation-induced changes of amplitudes of Fe^{3+} ion resonances at $g = 4.3$ as a function of glass composition [46].

5.3 Some general comments on processes of defect formation and recombination

Different types of trapped holes and electrons being simultaneously involved in trapping and detrapping reactions have been considered above. The occurrence of an isobestic point in figure 8b together with the corresponding time dependencies suggest simple recombination reactions taking place at the optically bleaching of sample BS. But one has to consider different types of trapped electrons: those trapped by Fe^{3+}, those causing the asymmetric resonance at $g = 1.955$, and those, responsible for the absorption band at 300 nm. Otherwise one should take into account that different types of holes trapped at nonbridging oxygens contribute to the ESR resonance at $g' = 2$. Unfortunately, it is not known how many optical absorption bands these centres cause.

Despite of the complex spectroscopic findings it is possible to get some insight into the radiation chemistry of sample BS. γ irradiation led to the formation of $Si-O^-/h^+$ and simultaneously trapping of electrons at Fe^{3+} ions. In addition, further types of trapped electrons could be detected. Subsequent optical bleaching did discover neither differences in the kinetics of recombination of $Si-O^-/h^+$ and electron centres ($g' \approx 1.955$) nor concerning the decay of optical absorption (figures 8a to d). But, thermal treatment of γ-irradiated samples brought about differences concerning the physical nature of the traps. It can be concluded from the results given in figures 9a to c that thermally (200 °C) stimulated reactions involve $Si-O^-/h^+$ centres and part of the electrons formerly trapped by Fe^{3+} ions (figure 9c: increase of absorption below 280 nm on temperature treatments). The result that Fe^{3+} ions can easily deliver the electrons trapped during γ irradiation before agrees with the in-

terpretation given in [53]. There it was stressed that trapping of electrons by Fe^{3+} did not lead to "real" Fe^{2+} ions but to so-called $(Fe^{3+})^-$ species. Otherwise, the fact that even after temperature treatment at 480 °C the absorbance below 280 nm did not reach the initial value again shows that the thermal stability, hence trap depth, of these $(Fe^{3+})^-$ species is characterized by a distribution broader than that of the $Si-O^-/h^+$ centres.

Two main groups of results were described above with respect to photochemically induced processes: first, interaction of glasses with light of an excimer laser (248 nm) could, depending on the repetition rate, cause formation or stimulated reaction of paramagnetic centres, and second, optical post-processing, i.e., exposure of γ-irradiated samples to the light of an Hg(Xe) lamp caused recombination of radiation-induced defects. Otherwise, exposure of nonirradiated samples kept at 77 K to this kind of intense UV and visible light did not lead to the formation of defects stable at room temperature.

It turns out that the concentration of defects depends on the repetition rate of the laser which can be explained by the combined action of optical and thermal effects. The energy of the 248 nm photons is high enough to cause defect formation as evidenced by ESR at low repetition rates. Knowledge of the optical absorption, which shows $Fe^{3+}-O$ charge transfer bands in this region, supports the idea that the defect formation is initiated by irreversible interaction of the laser light with Fe^{3+} ions co-ordinated by oxygen. But at higher repetition rates more energy is absorbed by the sample within a short period of time leading to optically stimulated reaction of the intermediates and local heating. As was shown before [51], $Si-O^-/h^+$ and Zn^+ centres possess different thermal stabilities[3]. Thus, the dependence of their ratio on the repetition rate of the laser can be explained by selective thermal bleaching effects.

The optical bleaching at 77 K with the light of an Hg(Xe) lamp can also be accompanied by local heating of the sample via optical absorption processes. But the observed differences concerning thermal and optical bleaching of γ-irradiated samples show that optically induced processes are dominating in the respective experiments performed here.

6. Summary and conclusions

Examining irradiated silicate and aluminosilicate glasses by means of optical and ESR spectroscopy as well as pulse radiolysis the following conclusions can be drawn:
a) Čerenkov radiation and stimulated emission can separately be detected on the time scale of microseconds.
b) The maximum of induced optical absorption observable on the time scale of microseconds appears at longer wavelength than that detected under stationary

---

[3] Thermal stability should be understood in terms of different rate constants for thermally stimulated reactions as already described in section 4.3.

conditions hours or days after the irradiations. This result is of practical importance if glassy optical components are exposed to high-energy radiation during use.

c) Up to now ESR and optical spectroscopy essentially provide complementary information. Study of influence of chemical composition and of thermal as well as of optical bleaching behaviour did only for selected cases allows one to mutually assign induced optical absorption bands and ESR resonances.

d) The glassy state is not only reflected by large distributions of ESR and optical parameters but also by broad distributions of thermal and photochemical stabilities of the radiation-induced colour and paramagnetic centres.

*

7. References

[1] Wong, J.; Angell, C.A.: Glass. Structure by spectroscopy. New York: Dekker, 1976. p. 612–659.

[2] Levy, P. W.: Overview of nuclear radiation damage processes: phenomenological features of radiation damage in crystals and glasses. SPIE **541** (1985) p. 2–24.

[3] Silin, A. R.: Light-induced ionic processes in optical oxide glasses. J. Non-Cryst. Solids **129** (1991) p. 40–45.

[4] Kanofsky, S.; Gershman, V.; Rosen, W.: Radiation effects on the components of optical LAN systems. SPIE **1791** (1992) p. 164–176.

[5] Berthold III, W. : Overview of prototype fiber optic sensors for future application in nuclear environments. SPIE **2425** (1994) p. 74–83.

[6] Rajaram, M.; Friebele, E. J: Effects of radiation on the properties of low thermal expansion coeffcient materials: A review. J. Non-Cryst. Solids **108** (1989) p. 1–17.

[7] Zhu, Z.; Jung, P.: Irradiation induced dimensional changes in ceramics. Nucl. Instrum. Methods Phys. Res. **B 91** (1994) p. 269–273.

[8] Farmer, V. R.: A review of reliability and quality assurance issues for space optics systems. SPIE **1761** (1992) p. 14–24.

[9] Speit, B.; Rädlein, E.; Frischat, G. H. et al. : Radiation resistant optical glasses. Nucl. Instrum. Methods Phys. Res. **B65** (1992) p. 384–386.

[10] Henschel, H.: Radiation hardness of present optical fibres. SPIE **2425** (1994) p. 21–31.

[11] Zmuda, W.; Pentrack, D.; Bulcock, W. R. et al.: In-situ measurements of the effects of neutron irradiation on polarization maintaining fiber. SPIE **1791** (1992) p. 329–335.

[12] Hillrichs, G; Dressel, M.; Hack, H. et al.: Transmission of XeCl excimer laser pulses through optical fibers – dependence on fiber and laser parameters. Appl. Phys. **B54** (1992) p. 208–215.

[13] Weeks, R. A.; Magrude III, R. H.; Wang, P. W.: Some effects of 5 eV photons on defects in SiO_2 J. Non-Cryst. Solids **149** (1992) p. 122–136.

[14] Dooryhee. E.; Langevin, Y.; Borg, J. et al.: Characterization of defects formed in amorphous SiO_2 by high energy ions using electron spin resonance and optical spectroscopy. Nucl. Instrum. Methods Phys. Res. **B32** (1988) p. 264–267.

[15] Dianov, E. M.; Kornienko, L. S.; Rybaltovskii, S. O. et al.: Unstable radiation colour centres in pure silica fibres: the nature and properties. SPIE **2425** (1994) p. 148–154.

[16] Buchmayer, G.; Rädlein, E.; Frischat, G. H.: Paramagnetic centres in glasses induced by low earth orbit space radiation. J. Non-Cryst. Solids **204** (1996) no. 3, p. 253–259.

[17] Fabian, H.; Grzesik, U.; Wörner, K.-H. et al.: Radiation resistance of optical fibers correlation between UV-attenuation and radiation induced loss. SPIE **1791** (1992) p. 297–304.

[18] Dutt, D. A.; Higby, P. L.; Griscom, D. L.: An electron spin resonance study of X-irradiated calcium aluminosilicate glasses. J. Non-Cryst. Solids **130** (1991) p. 41–51.

[19] Ezz-Eldin, F. M.; Kashif, I.; El-Batal, H. A.: Some physical properties of gamma-irradiated alkali-silicate glasses. Radiat. Phys. Chem. **44** (1994) no. 1/2, p. 39–43.

[20] El-Batal, H. A.; Ezz-Eldin, F. M.; Elalaily, N. A.: Effect of gamma-rays on electrical conductivity of some selected alkali-alkaline earth-silicate glasses. Nucl. Sci. J. **31** (1994) no. 2, p. 73–82.

[21] Ehrt, D.; Vogel, W.: Radiation effects in glasses. Nucl. Instrum. Methods Phys. Res. **B 65** (1992) p. 1–8.

[22] Dickinson, J. T.; Langford, S. C.; Jensen, L. C.: Simultaneous bombardment of wide bandgap materials with UV excimer irradiation and keV elektrons. Lect. Notes Phys. (Laser Ablation Mech.Appl.) **389** (1991) p. 301–309.

[23] Stößer, R.; Nofz, M.: Excimer laser generation and stimulated decay of paramagnetic species in inorganic glasses. (In Prep.)

[24] Janata, E.: Instrumentation of kinetic spectroscopy. Pt. 12. Software for data acquisition in kinetic experiments. Radiat. Phys. Chem. **44** (1994) no. 5, p. 449–454.

[25] Janata, E.: Pulse radiolysis as a tool in small particle research. Radiat. Phys. Chem. **47** (1996) no. 1, p. 29–32.

[26] Janata, E.; Gutsch, W.: Instrumentation of kinetic spectroscopy. Pt. 15. Injector parts generators for electron accelerators, part 3. Radiat. Phys. Chem. **51** (1998) no. 1, p. 65–71.

[27] Nofz, M.; Stößer, R.; Wihsmann, F. G.: Paramagnetic centres in glasses of the system $CaO-Al_2O_3-SiO_2$. Phys. Chem. Glasses **31** (1990) no. 2, p. 57–63.

[28] Weissmantel, C.; Lenk, R.; Forker, W. et al. (eds.): Kleine Enzyklopädie Atom. Leipzig: Bibliogr. Inst., 1970. p. 182.

[29] Schpolski, E. W.: Atomphysik. T.I. 19. Aufl. Leipzig (et al.) Barth, 1993. p. 245–253.

[30] Falbe, J.; Regitz, M. (eds.): Römpp Chemie-Lexikon. Bd. 1. 9. Aufl. Stuttgart: Thieme, 1995. p. 624.

[31] Nofz, M.; Stösser, R.; Reich, C. et al.: On the multifarious results of interaction between amorphous materials and irradiation of different energies – a spectroscopic study. In: Akçakaya, R.; Erinç, N.; Albayrak, G. et al. (eds.): Proc. International Symposium on Glass Problems, Istanbul (Turkey) 1996. Vol. 1. Instanbul: ŞTŞECAM, 1996, p. 94–100.

[32] Nofz, M.; Stösser, R.; Reich, C. et al.: Spectroscopic characterization of radiation induced transient and long-living defects in doped silicate glasses. In: Fundamentals of Glass Science and Technology. Växjö (Sweden) 1997. p. 652–657.

[33] Stösser, R.; Nofz, M.; Momand, J.-A. et al.: Correspondence between physical parameters of glasses and defect formation under the influence of high energy irradiation. In: Schaeffer, H. A. (ed.): Proc. 3rd Conference European Society of Glass Science and Technology. Fundamentals of Glass Science and Technology, Würzburg 1995. (Glastech. Ber. Glass Sci. Technol. **68 C1** (1995) p. 188–195.

[34] Griscom, D. L.: Electron spin resonance studies of trapped hole centers in irradiated alkali silicate glasses: A critical comment on current models for HC_1 and HC_2. J. Non-Cryst. Solids **64** (1984) p. 229–247.

Glastech. Ber. Glass Sci. Technol. 72 (1999) No. 3

89

[35] Cases, R.; Griscom, D. L.: On the structure of defect centers in γ-irradiated alkali silicate glasses. Nucl. Instrum. Methods Phys. Res. **B1** (1984) p. 503—510.

[36] Stösser, R.; Nofz, M.; Lück, R.: EPR on glasses and silicates: Some order/disorder phenomena observed in $CaO/Al_2O_3/SiO_2$ and related systems. Exp. Tech. Phys. **36** (1988) no. 4/5, p. 327—337.

[37] Nofz, M.: Interpretation empirischer Zusammenhänge zwischen Zusammensetzung und physikalischen Eigenschaften von Alumosilikatgläsern auf der Basis eines Strukturmodells. Zentralinstitut f. Anorganische Chemie, Akademie d. Wissenschaften d. DDR, Berlin, thesis 1990.

[38] Bartoll, J.: Spektroskopie und Strahlenchemie ungeordneter Festkörper mit Eisen- und Mangan-Dotierung. Humboldt-Universität, Berlin, thesis 1998.

[39] Völkel, G.; Pöppl, A.; Voigtsberger, B.: Investigation of the oxygen vacancy balance in ZnO ceramics by means of EPR. phys. stat. sol. **(a) 109** (1988) p. 295—299.

[40] Steele, F. N.; Douglas, R. W.: Some observations on the absorption of iron in silicate and borate glasses. Phys. Chem. Glasses **6** (1965) no. 6, p. 246—252.

[41] Ades, C.; Toganidis, T.; Traverse, J. P.: High-temperature optical spectra of soda—lime—silica glasses and modelization in view of energetic applications. J. Non-Cryst. Solids **125** (1990) p. 272—279.

[42] Hart, E. J.; Anbar, M.: The hydrated electron. J. Wiley & Sons, New York (et al.): Wiley, 1979. p. 41.

[43] Dutt, D. A.; Highby, P. L.; Merzbacher, C. I. et al.: Radiation induced trapped hole centers in calcium aluminosilicate glasses. Ceramic Transactions **28** (1992) p. 111—122.

[44] Smets, B. M. J.; Lommen, T. P. A.: The incorporation of aluminium oxide and boron oxide in sodium silicate glasses, studied by x-ray photoelectron spectroscopy. Phys. Chem. Glasses **22** (1981) no. 6, p. 158—162.

[45] Griscom, D. L.: Electron spin resonance in glasses. J. Non-Cryst. Solids **40** (1980) p. 211—272.

[46] Stösser. R.; Nofz, M.: Unpubl. res.

[47] Stösser, R.; Nofz, M.; Herrmann, W.: ESR evidence for trapping of electrons in glass. In: Fundamentals of Glass Science and Technology 1993. Proc. 2nd Conference European Society of Glass Science and Technology, Venice (Italy) 1993. Suppl. to Riv. Stn. Sper. Vetro **23** (1993) p. 523—526.

[48] Friebele, E. J.; Griscom, D. L.: Radiation effects in glass. In: Tomozawa, M.; Doremus, R. (eds.): Glass II. New York, London: Academic Press, 1979. p. 257—351. Treatise on Materials Science and Technology. Vol. 17.)

[49] Glebov, L. B.; Dokuchaev, V. G.; Petrov M. A. et al.: Absorption spectra of color centers in alkali silicate glasses. Sov. J. Glass Phys. Chem. **16** (1990) no. 1, p. 31—38.

[50] Friebele. E. J.; Higby, P. L.; Tsai, T. E.: Radiation-induced (optical absorption in amorphous silicas prepared by different techniques. In: Weeks, R. A.; Kinser, D. L. (eds.): Effects of modes of formation on the structure of glasses. Proc. 2nd Int. Conf., Nashville, TN (USA) 1987. Aedermannsdorf: Trans Tech. Publ., 1987. p. 203—212.

[51] Nofz, M.; Stösser, R.; Scholz, G. et al.: Time and dose dependent effects of high-energy radiation on glasses. Presented at: XVIII International Congress on Glass, San Francisco, CA (USA) 1998.

[52] Popp, P.; Nofz, M.; Stösser, R.: Combined optical, ESR spectroscopic and kinetic studies of γ-radiation induced defects in glasses. In: Fundamentals of Glass Science and Technology 1993. Proc. 2nd Conference European Society of Glass Science and Technology, Venice (Italy) 1993. Suppl. to Riv. Stn. Sper. Vetro **23** (1993) p. 519—522.

[53] Arbuzov, W. I.; Nikolaev, Ju. P.; Raaben, E. L. et al.: Spektralno-ljumineszentnije i fotochimischeskie swoistwa silikatnych stekol s Fe^{2+} i Fe^{3+}. (Orig. Russ.). Fiz. Chim. Stekla **13** (1987) no. 4, p. 625—628.

■ 0399P003

Addresses of the authors:

M. Nofz, C. Reich
Bundesanstalt für Materialforschung und -prüfung
Außenstelle Adlershof, Labor V. 43 „Glas und Glaskeramik"
Rudower Chaussee 5, D-12489 Berlin

R. Stösser, J. Bartoll
Institut für Chemie, Humboldt-Universität Berlin
Hessische Straße 1—2, D-10115 Berlin

E. Janata
Hahn-Meitner-Institut
Bereich Physikalische Chemie
Glienicker Straße 100
D-14109 Berlin